Benha University
Benha Faculty of Engineering
Basic Engineering Sciences Department

Synthesis and Investigation of Physical Properties of Some Nanocomposites

A thesis submitted in partial fulfillment of the requirements of the M.Sc. in Engineering Physics.

By

Mohamed Okil Shawky Abdel-Wahab

B.Sc. of Engineering & Technology in Electrical Engineering Technology – Benha Faculty of Engineering – Benha University (2011)

Supervised by

Assoc. Prof. Dr. *Samaa Imam Mahmoud El-Dek*

Department of Materials Science and Nanotechnology

Faculty of Post Graduate Studies for Advanced Sciences

Beni-Suef University

Dr. *Mohamed Mostafa Mohamed Elfaham*

Department of Basic Engineering Sciences

Benha Faculty of Engineering

Benha University

Benha 2019

The undersigned committee had examined the thesis entitled

Synthesis and Investigation of Physical Properties of Some Nanocomposites

Presented by

Mohamed Okil Shawky Abdel-Wahab

B.Sc. of Engineering & Technology in Electrical Engineering Technology – Benha Faculty of Engineering – Benha University (2011)

a candidate for the degree of

M.Sc. in Engineering Physics

and hereby certify that it is worthy of acceptance

Prof. Dr.	**(Committee Chairperson)**
Gamal Abdel-Naser Madbouly	
Professor of Physics	
Former Vice President of Cairo University	
Faculty of Sciences, Cairo University	
Assoc. Prof. Dr.	**(Committee Member)**
Mahmoud Fathy Mahmoud Hassan	
Associate Professor of Physics	
Benha Faculty of Engineering, Benha University	
Assoc. Prof. Dr.	**(Committee Member)**
Samaa Imam Mahmoud El-dek	
Associate Professor of Materials Science and Nanotechnology	
Faculty of Postgraduate studies for Advanced Sciences, Beni-Suef University	
Accepted from Basic Engineering Sciences Department	
Prof. Dr.	**(Department Chairman)**
Elsayed Ali Ibrahim Fouad	
Accepted from the Postgraduate Affairs	
Prof. Dr.	**(Vice Dean for Postgraduate Studies)**
Hesham Mohamed El-Batsh	
Accepted from the Faculty	
Prof. Dr.	**(Dean of the Faculty)**
Aref Mohamed Soliman	

The undersigned committee had examined the thesis entitled

Synthesis and Investigation of Physical Properties of Some Nanocomposites

Presented by

Mohamed Okil Shawky Abdel-Wahab

B.Sc. of Engineering & Technology in Electrical Engineering Technology – Benha Faculty of Engineering – Benha University (2011)

a candidate for the degree of

M.Sc. in Engineering Physics

and hereby certify that it is worthy of acceptance

Prof. Dr. **(Committee Chairperson)**

Gamal Abdel-Naser Madbouly

Professor of Physics

Former Vice President of Cairo University

Faculty of Sciences, Cairo University

Assoc. Prof. Dr. **(Committee Member)**

Mahmoud Fathy Mahmoud Hassan

M.F.M. Hassan

Associate Professor of Physics

Benha Faculty of Engineering, Benha University

Assoc. Prof. Dr. **(Committee Member)**

Samaa Imam Mahmoud El-dek

Samaa

Associate Professor of Materials Science and Nanotechnology

Faculty of Postgraduate studies for Advanced Sciences, Beni-Suef University

---

Accepted from Basic Engineering Sciences Department

Prof. Dr. **(Department Chairman)**

Elsayed Ali Ibrahim Fouad

Accepted from the Postgraduate Affairs

Prof. Dr. **(Vice Dean for Postgraduate Studies)**

Hesham Mohamed El-Batsh

H.E. Batsh

Accepted from the Faculty

Prof. Dr. **(Dean of the Faculty)**

Aref Mohamed Soliman

ACKNOWLEDGEMENTS

*First and foremost, all praises to my Allah for the strengths and His blessing in completing this thesis (**Thanks to my Allah**).*

*Words are insufficient in offering my thanks to my advisor who had been a source of inspiration **Assoc. Prof. Dr. Samaa Imam Mahmoud El-Dek**, Professor of Materials Science and Nanotechnology, Faculty of Post Graduate Studies for Advanced Sciences, Beni-Suef University, for her able guidance and useful suggestions, which helped me in completing this work.*

*I wish to express my deep sense of gratitude to my guide, **Dr. Mohamed Mostafa Mohamed Elfaham**, Lecturer of Physics, Benha Faculty of Engineering, Benha University, for his assistance in this work.*

*Finally, I would like to thank my family for their continuous support and encouragement. For my parents, **Okil** and **Howaida**, who raised me with a love of science and supported me in all my pursuits. I am particularly grateful for my loving, supportive, encouraging, and patient wife **Radwa** and to my beautiful baby **Karma** without your support, sound, and smile I could never have accomplished this work.*

Mohamed Okil

TABLE OF CONTENTS

LIST OF ABBREVIATIONS AND SYMBOLS

List of Abbreviations:

Al–LH	Aluminum layered hydroxides
MWCNTs	Multiwalled carbon nanotubes
CVD	Chemical vapor deposition
XRD	X-ray diffraction
FTIR	Fourier transformer infrared
FESEM	Field emission scanning electron microscopy
HRTEM	High resolution transmission electron microscopy
EDX	Energy-dispersive X-ray
BET	Brunauer-Emmett-Teller
BJH	Barrett-Joyner-Halenda
TGA	Thermal gravimetric analysis
DSC	Differential scanning calorimetry

List of Symbols:

x	The weight percent
λ	The X-ray target wavelength
d	The interplanar spacing
(hkl)	The miller indices of a plane
a, b, c	The lattice parameters
V	The unit cell volume
ρ_{th}	The X-ray density
ρ_{exp}	The experimental density
P	The porosity
Z	The number of molecules per unit cell

$\boldsymbol{M}$	The molecular weight
$\boldsymbol{N_A}$	The Avogadro's number
$\boldsymbol{D}$	The average crystallite size
$\boldsymbol{V_L}$	The longitudinal velocity
$\boldsymbol{V_S}$	The shear velocity
$\boldsymbol{L}$	The longitudinal modulus
$\boldsymbol{G}$	The rigidity modulus
$\boldsymbol{\sigma}$	The Poisson's ratio
$\boldsymbol{B}$	The bulk modulus
$\boldsymbol{E}$	The Young's modulus
$\boldsymbol{H_v}$	The calculated Vickers microhardness

LIST OF FIGURES

LIST OF TABLES

SUMMARY OF THE PAPER

Multiwalled carbon nanotubes (MWCNTs) has been synthesized using chemical vapor deposition (CVD) method. Al – Layered Hydroxide (Al–LH) and MWCNTs nanocomposites; (1-*x*) Al–LH + (*x*) MWCNTs, $0.0 \leq x \leq 1$; have been synthesized using citrate nitrate assisted hydrothermal technique. The crystal structure and the functional groups of the prepared samples were examined using X-ray diffraction (XRD) and Infrared spectroscopy (FTIR) respectively. Their layered structure seemed under the high-resolution transmission electron microscopy (HRTEM), and the morphology was observed using field emission scanning electron microscopy (FESEM). Moreover, the synthesized nanocomposites were further characterized using Zeta potential and size analysis and Brunauer–Emmett–Teller (BET) surface area which showed their different characteristics as the MWCNTs content is changed. Thermal gravimetric analysis assured the thermal stability of the nanocomposites over the temperature from room up to 480 °C depending on the MWCNTs content. The obtained results revealed the improvement of all mechanical properties with the increase of MWCNTs content.

RESEARCH PLAN

For the degree of M.Sc. in Engineering Physics

Candidate Name: Eng. Mohamed Okil Shawky Abdel-Wahab
Demonstrator – Benha Faculty of Engineering – Benha University

Title of the research:

"Synthesis and Investigation of Physical Properties of Some Nanocomposites"

Abstract:

Development of nanomaterials is one of the most important advances in science. Nanomaterials are substances that have at least one dimension in the nanoscale scope, which gives them extraordinary physical and chemical properties. Layered nanocomposites represent a specific class of multi-purpose materials that has obtained numerous considerations in recent years. Theses nanocomposites allow the progress of innovative applications in industry in addition to representing an inventive alternative to the research for new materials. The potential usage of layered nanocomposites encompasses photovoltaic devices, intelligent membranes, biochemical and chemical detectors, new catalysts, separation devices, smart microelectronic devices in addition to some materials merging ceramics and polymers, etc. For layered nanocomposites, strong interactions and homogeneous dispersion with the matrices are the most important problem. Moreover, no studies have been conducted on the synthesis of Al–LH and MWCNTs nanocomposites. Motivated by this, we will focus our work on the synthesis of Al–LH/MWCNTs nanocomposites and investigation of their physical properties for potential applications.

Research Plan:

1. Preparation of all nanocomposites using the hydrothermal technique.
2. The crystal structure and the functional groups of the prepared samples will be examined using X-ray diffraction (XRD) and Infrared spectroscopy (FTIR) respectively.
3. The microstructure will be examined using Transmission Electron Microscopy.
4. The morphology will be depicted using Field Emission Scanning Electron Microscopy.
5. Zeta potential investigation will be carried out for all nanocomposites.
6. BET surface area analysis will be carried out for all nanocomposites.
7. Physical properties will be investigated for all nanocomposites.

Supervisors:

Assoc. Prof. Dr. Samaa Imam Mahmoud El-Dek ( )
Associate Professor of Materials Science and Nanotechnology
Faculty of Postgraduate Studies for Advanced Sciences, Beni-Suef University

Dr. Mohamed Mostafa Mohamed Elfaham ( )
Lecturer of Physics, Benha Faculty of Engineering, Benha University

Research Plan:

1. Preparation of all nanocomposites using the hydrothermal technique.
2. The crystal structure and the functional groups of the prepared samples will be examined using X-ray diffraction (XRD) and Infrared spectroscopy (FTIR) respectively.
3. The microstructure will be examined using Transmission Electron Microscopy.
4. The morphology will be depicted using Field Emission Scanning Electron Microscopy.
5. Zeta potential investigation will be carried out for all nanocomposites.
6. BET surface area analysis will be carried out for all nanocomposites.
7. Physical properties will be investigated for all nanocomposites.

Supervisors:

Assoc. Prof. Dr. Samaa Imam Mahmoud El-Dek (Samaa)
Associate Professor of Materials Science and Nanotechnology
Faculty of Postgraduate Studies for Advanced Sciences, Beni-Suef University

Dr. Mohamed Mostafa Mohamed Elfaham (Moh. El. Fahamy)
Lecturer of Physics, Benha Faculty of Engineering, Benha University

CHAPTER 1 (JOURNAL PAPER)

“Fascinating thermo-mechanical features of layered hydroxides/ MWCNTs nanocomposites”

Journal of Alloys and Compounds vol.788 (2019)
Pages 912-924

Journal of Alloys and Compounds 788 (2019) 912–924

Contents lists available at ScienceDirect

Journal of Alloys and Compounds

journal homepage: http://www.elsevier.com/locate/jalcom

Fascinating thermo-mechanical features of layered hydroxides/MWCNTs nanocomposites

M. Okil [a], Mohamed M. ElFaham [a], S.I. El-dek [b, *]

[a] Basic Engineering Sciences Department, Benha Faculty of Engineering, Benha University, Egypt
[b] Materials Science and Nanotechnology Department, Faculty of Postgraduate Studies for Advanced Sciences (PSAS), Beni-Suef University, Egypt

ARTICLE INFO

Article history:
Received 6 November 2018
Received in revised form
29 January 2019
Accepted 18 February 2019
Available online 22 February 2019

Keywords:
Layered hydroxides
MWCNTs
Nanocomposites
Thermal stability
Mechanical properties
Ultrasonic velocity

ABSTRACT

Multiwalled carbon nanotubes (MWCNTs) has been synthesized using chemical vapor deposition (CVD) method. Al − Layered Hydroxide (Al–LH) and MWCNTs nanocomposites; (1-*x*) Al–LH + (*x*) MWCNTs, $0.0 \leq x \leq 1$; have been synthesized using citrate nitrate assisted hydrothermal technique. The crystal structure and the functional groups of the prepared samples were examined using X-ray diffraction (XRD) and Infrared spectroscopy (FTIR) respectively. The layered structure seemed under the high-resolution transmission electron microscopy (HRTEM), and the morphology was observed using field emission scanning electron microscopy (FESEM). Moreover, the synthesized nanocomposites were further characterized using Zeta potential, size analysis and Brunauer– Emmett–Teller (BET) surface area which showed their different characteristics as the MWCNTs content is changed. Thermal gravimetric analysis assured the thermal stability of the nanocomposites over the temperature from room up to 480 °C depending on the MWCNTs content. The obtained results revealed the improvement of all mechanical properties with the increase of MWCNTs content.

1. Introduction

Development of nanomaterials is one of the most important advances in science. Nanomaterials are substances that have at least one dimension in the nanoscale scope, which gives them extraordinary physical and chemical properties, as well as quantum effect, high-reactivity, and high-to-volume ratio. Even though nanomaterials can be manufactured in one, two or three dimensions, dual dimension nanosheets has extremely fascinated scientists because of their incomparable interaction properties [1,2].

Layered hydroxides, with their adapted performance and excellent physio-chemical properties, offer wide applications in numerous fields, as water treatment, anticorrosion agent, like a catalyst, flame retardants, sensors and electrodes in addition to its usage in drug delivery systems [3–6]. They are made up of nanolayers with unlimited two-dimensional layers with a thickness in the nanoscale and contribute to large-scale applications in different fields. These host layered materials can be characterized as layered double hydroxides (LDH) and layered hydroxide salts (LH) [7,8].

Layered nanocomposites represent a specific class of multipurpose materials that has obtained numerous considerations in recent years. The specialized structure of nanocomposites develops a synergistic influence among the organic and nonorganic parts, creating compounds with dissimilar physical or chemical properties compared with the isolated components. Theses nanocomposites allow the progress of innovative applications in industry in addition to representing an inventive alternative to the research for new materials. The potential usage of layered nanocomposites encompasses photovoltaic devices, intelligent membranes, biochemical and chemical detectors, new catalysts, separation devices, smart microelectronic devices in addition to some materials merging ceramics and polymers, etc. [9–12].

MWCNTs gained more attention worldwide in the last decades due to their superior chemical stability, excellent electrical conductors, strength, stiffness, unique structural, high thermal conductivities in addition to their full range of potential applications in nanoelectronics, optics, sensors and nanocomposites [13,14]. Moreover, they can be reacted and treated using carbon-rich chemistry as its composition consists of a pure carbon polymer. Therefore, it may allow for many innovative applications in materials, electronic engineering, chemical processing, and energy management due to the possibility of its structural modification

* Corresponding author.
E-mail address: samaa@psas.bsu.edu.eg (S.I. El-dek).

https://doi.org/10.1016/j.jallcom.2019.02.218
0925-8388/

and solubility optimization [15].

For both layered hydroxides and CNTs nanofillers, strong interactions and homogeneous dispersion with the matrices are the most important problem. Many investigations have been done on modification and dispersion of LDH [16–18] and CNTs [19–21] in polymeric matrices. However, considering special structure and properties of LDH and CNTs, it is very interesting to prepare LDH/CNTs nanocomposites for their promising applications in the field of electrocatalyst [22], hydrogen storage device [23], photodegradation of dye etc. [24]. Recently, this type of nanocomposites has been synthesized by hydrothermal method [25,26], co-precipitation method [22,24], dry grinding of CNT and LDH [27] and wet mixing [28]. Moreover, no studies have been conducted on the synthesis of Al–LH and MWCNTs nanocomposites. Motivated by this, we focused our work on the preparation of Al–LH/MWCNTs nanocomposites using citrate nitrate assisted hydrothermal technique and investigation of their physical properties for potential applications.

2. Experimental details

2.1. Synthesis of Al–LH nanoparticles

Al $(NO_3)_3 \cdot 6H_2O$ was used to prepare the layered hydroxide by adding citric acid to metal nitrate with a ratio of 1:1. The reactants were mixed in bi-distilled water under thorough stirring. The pH value was adjusted to 7 using some droplets of ammonia solution. The mixture was then transferred on a hot plate until drying where a fluffy grey powder was observed to grow in the beaker. This powder was collected, grinded and then transferred to a Teflon-lined stainless-steel autoclave.

2.2. Synthesis of MWCNTs

2.2.1. Chemicals

MWCNTs were synthesized using a chemical vapor deposition technique, using a tube furnace of 45 mm diameter and 60 cm length quartz tube. All chemicals were utilized without further purification.

2.2.2. Preparation of Fe/Co/$CaCO_3$ supporting catalyst

The supporting catalyst for MWCNTs production was prepared according to the reported method by Schwarz et al. [29] when an appropriate quantity of calcium carbonate was grinded in a ball mill for 15 h to minimize the particle size and increase the surface area. After that, calcium carbonate, ferric nitrate Fe $(NO_3)_3 \cdot 9H_2O$ and cobalt nitrate Co $(NO_3)_2 \cdot 6H_2O$ were mixed together with ratios of 95%, 2.5%, 2.5% respectively. The mixture was then milled again for 2 h. After that, it was made in the form of paste by adding drops of bi-distilled water and homogeneously mixed, dried at 120 °C overnight, and then grinded to get fine powder of supporting catalyst [30].

2.2.3. Preparation of MWCNTs

Chemical vapor deposition method was utilized for the synthesis of MWCNTs (see Fig. 1), in which acetylene with iron and cobalt mixture in an inert gas atmosphere is presented into the reaction chamber. During which, nanotubes were produced on the substrate by the decomposition of the hydrocarbon at temperature 600–900 °C at atmospheric pressure. The dimensions of the formed nanotubes are related to the size of the metal particle used. This technique offers more control over the length and structure of the formed nanotubes compared with arc and laser methods.

This process can also be scaled up to produce industrial quantities of MWCNTs. According to the reported method by Bahgat et al. [30], MWCNTs was prepared as follow, 2 g of the supporting catalyst was placed in an alumina boat and introduced into the cylindrical quartz tube fitted inside a tube furnace and adjusted at 600 °C and the catalyst was preheated for 10 min in the presence of nitrogen gas flow by a rate of 90 ml/min. After catalyst heating, a flow of acetylene gas was allowed to pass over the catalyst through the quartz tube at a flow rate of 90 ml/min for 40 min. After the desired time, the acetylene flow was stopped and the product was cooled to room temperature.

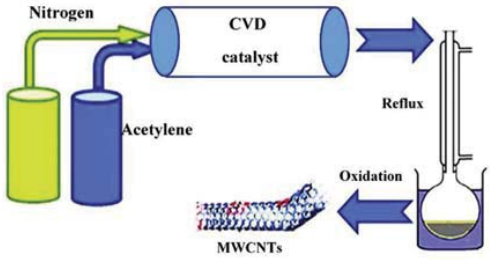

Fig. 1. Synthesis of MWCNTs using CVD technique.

2.2.4. Purification and functionalization of MWCNTs

The extremely large surface area leads to a strong tendency to form agglomerates. Surface functionalization helps in stabilizing the dispersion since it can prevent re-aggregation of nanotubes and also leads to coupling of MWCNTs with the polymeric matrix. Covalent functionalization of MWCNTs can be achieved by introducing some functional groups on defect sites of MWCNTs by using oxidizing agents such as strong acids, which results in the formation of carboxylic or hydroxyl groups (–COOH, –OH) on the surface of nanotubes. This type of functionalization is known as defect group functionalization [30].

The functionalization process was performed as follow:

1. Typically, 30 ml of conc. HNO_3 and 10 ml of conc. H_2SO_4 were injected into a 250 ml flask loaded with 5 g phosphorous pentoxide and 10 g of as obtained MWCNTs.
2. The mixture was refluxed at 350 °C for 2 h to obtain MWCNTs suspended solution.
3. The solution was washed with deionized water until pH of filtrate approached that of distilled water.
4. The final step is drying at 50 °C overnight to obtain carboxylated MWCNTs (MWCNTs–COOH).

2.3. Synthesis of the Al–LH and MWCNTs nanocomposites

Al–LH and MWCNTs nanocomposites were synthesized using the hydrothermal method [31]. In a typical procedure, the constituents were prepared with the weights as shown in Table 1. These nanocomposites were prepared using sonochemical method

Table 1
The constituents weight percent of the prepared nanocomposites.

x (wt.%)	MWCNTs (*x*)	Al–LH (1-*x*)
0	0	100
2.5	2.5	97.5
5	5	95
7.5	7.5	92.5
100	100	0

[32]. Each component was mixed with 20 ml of double distilled water. Al–LH was well dispersed using Probe Sonication (Ultrasonic Processor - Sonics & Materials, Inc. - Probe diameter is 5–8 mm). MWCNTs were well dispersed using Bath Sonication (Elma Sonic – Elma – S30H). They were then mixed and dispersed using Bath Sonication for 30 min. The prepared solution was then poured into the Teflon-lined stainless-steel autoclave with 100 ml capacity and heat treated at 160 °C for 24 h. The autoclave chambers were air-cooled to room temperature after the completion of the reaction. The formed precipitates were washed several times with double distilled water, and they were finally dried at 100 °C for 7 h in the air.

2.4. Characterizations

The crystalline phases and d-spacing of the investigated nanocomposites were examined by X-ray diffraction (202964 PANalytical Empyrean) using Cu Kα radiation (λ = 1.54060 Å) under the operating conditions of 30 mA and 40 kV. The scanning range was from 5° to 80° with a step size of 0.04° and a time per step of 0.5 s. The experimental density was determined by the immersion method using Archimedes' principle with toluene as a solvent. The infrared spectroscopic analysis was carried out using the KBr pellet technique on a Bruker (Vertex 70 FT-IR) spectrometer coupled to a RAM II FT-Raman module in the range from 4000 to 400 cm^{-1}. The microstructure was examined using high-resolution transmission electron microscopy (HRTEM) model JEOL-JEM 2100 (Japan) with an acceleration voltage of 200 kV. The morphology was depicted using a Quanta FEG 250 (Czechoslovakia) field emission scanning electron microscopy (FESEM) occupied with the energy-dispersive X-ray spectroscopy (EDX) systems. The zeta potential was measured by Zetasizer Nano-Zs90 (Malvern, UK). The N_2 adsorption-desorption isotherms were determined using Micromeritics-Tristar II (USA), with the samples degassed at 80 °C for 3 h under vacuum prior to the measurements. The specific surface area, pore-size distribution, and pore volume were estimated from the isotherms by the Brunauer-Emmett-Teller (BET) and Barrett-Joyner-Halenda (BJH) methods, respectively. Thermal gravimetric analysis (TGA) and differential scanning calorimetry (DSC) were performed on (SDT Q600 V20.9 Build 20) for the nanocomposites in the range from room temperature up to 700 °C using heating rate of 7 °C/min under nitrogen atmosphere. The longitudinal wave velocity V_L and shear velocity V_S through the nanocomposites were measured applying ultrasonic pulse-echo technique by using (GE model: USN60). The sound velocity was propagated along the direction of pressing using Y-cut (shear) or X-cut (longitudinal) transducer with the carrier frequency of 4 MHz. A timer recorded the signal transit time Δt through the sample. The sound velocity V was calculated using the equation: $V = \frac{L'}{\Delta t}$ [33] where L' is the round-trip distance traveled by sound. All velocity measurements in this study were carried out at room temperature, and at frequency 4 MHz. The measurement accuracy was ±0.5%.

3. Results and discussion

3.1. X-ray diffraction analysis (XRD)

Fig. 2: a–e shows the X-ray diffraction patterns of Al–LH, MWCNTs and their nanocomposites. As apparent from the figure, all diffraction peaks of Al–LH are indexed with the standard pattern for AlO (OH) reported in (ICDD card no. 04-010-5683). The reflections observed at 2θ = 14.45°, 28.13°, 38.31°, 45.79°, 49.08°, 51.51°, 55.19°, 60.55°, 64.08°, 64.98°, 67.64° and 71.99° correspond to the planes indexed as (020), (021), (130), (131), (002), (022), (151), (080), (132), (200), (171) and (152), respectively. The samples were formed in an orthorhombic crystal form with space group *Cmcm* as identified from the corresponding ICDD with 4 formula unit per unit cell. It is clear that the crystal structure prefers the growth in the b direction. With increasing the content of MWCNTs in the nanocomposite, the reflections are nearly similar with their respective ratios keeping the basic reflections of the MWCNTs hindered owing to their poor crystallinity as compared with the layered structure. Moreover, the observed peaks for MWCNTs at 2θ = 25.87°, 43.10°, and 65.68° correspond to the planes of (220), (301) and (002), respectively, as indexed from (ICDD card no. 01-083-3673). MWCNTs were formed in a tetragonal crystal form with space group *I*4/*mmm* as identified from the corresponding ICDD with 24 formula unit per unit cell. It is clear that the crystal structure prefers the growth in the a and b directions. From Fig. 2a–d, The XRD patterns exhibited sharp basic reflection series at relatively low 2θ angles indicating a well-crystallized structure for the prepared nanocomposites.

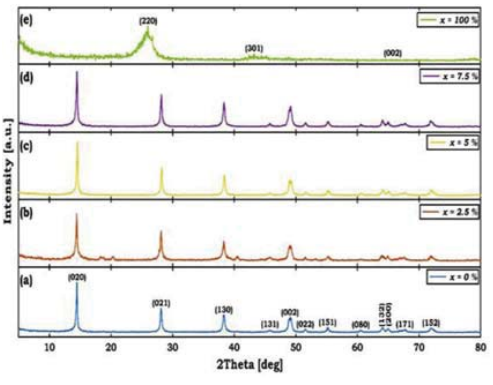

Fig. 2. (a–e): XRD patterns of (1-*x*) Al–LH + (*x*) MWCNTs nanocomposites with *x* = 0, 2.5, 5, 7.5 and 100 wt%.

The lattice parameters of the Al–LH were calculated based on the orthorhombic symmetry using the equation [34]:

$$\frac{1}{d^2} = \frac{h^2}{a^2} + \frac{k^2}{b^2} + \frac{l^2}{c^2}; \quad a \neq b \neq c \tag{1}$$

where: d, (hkl), a, b, and c are the interplanar spacing, the Miller indices of the plane, and the lattice parameters respectively. The unit cell volume and theoretical density were calculated using the equations [34]:

$$V = a \times b \times c \tag{2}$$

$$\rho_{th} = \frac{Z\,M}{N_A\,V} \tag{3}$$

where: V, ρ_{th}, Z, M, and N_A are the unit cell volume, the theoretical density, the number of molecules per unit cell, the molecular weight and Avogadro's number respectively.

The obtained data are reported in Table 2 together with those calculated for MWCNTs. The reported values are kept nearly constant from *x* = 0% up to *x* = 7.5% indicating the stability of the layered structure in addition to the minor changes caused by the small amount of MWCNTs. The lattice parameters of MWCNTs were

Table 2
The values of lattice parameters, Unit cell volume (V), X-ray density (ρ_{th}) experimental density (ρ_{exp}), porosity (P) and crystallite size (D) as a function x for the nanocomposites (1-x) Al–LH + (x) MWCNTs with $x = 0$, 2.5, 5, 7.5 and 100 wt%.

x (wt.%)	a (Å)	b (Å)	c (Å)	V (Å^3)	ρ_{th} (g/cm^3)	ρ_{exp} (g/cm^3)	P %	D (nm)
0	2.8749	12.2028	3.7026	129.89	3.07	1.62	47.23	32
2.5	2.8581	12.2799	3.7074	130.12	3.06	1.47	51.96	29
5	2.8893	12.0411	3.7048	128.89	3.09	2.23	27.83	43
7.5	2.8773	12.1611	3.7037	129.59	3.07	1.83	40.39	35
100	9.5351	9.5351	2.8431	258.48	1.85	–	–	23

calculated based on the tetragonal symmetry using the equation [34]:

$$\frac{1}{d^2} = \frac{h^2 + k^2}{a^2} + \frac{l^2}{c^2}; \quad a = b \neq c \tag{4}$$

where: d, (hkl), a, b, and c are the interplanar spacing, the Miller indices of the plane, and the lattice parameters respectively. The unit cell volume was calculated using the equation [34]:

$$V = a^2 \times c \tag{5}$$

where: V, a, and c are the unit cell volume and the lattice parameters respectively. The theoretical density was computed as mentioned above eq. (3) and the porosity was computed from the equation:

$$P = \left(1 - \frac{\rho_{exp}}{\rho_{th}}\right) \times 100 \tag{6}$$

where: ρ_{exp} is the experimental density and ρ_{th} is the X-ray density. The average crystallite size was calculated from the well-known Scherrer's formula for each phase separately [34]. The size ranged from 29 to 43 nm for the investigated nanocomposites and was 23 nm for MWCNTs.

3.2. Fourier transform infrared (FTIR)

Fig. 3 illustrates the FTIR spectra of Al–LH and MWCNTs and their nanocomposites. The spectrum of Al–LH exhibits bands at 3287 cm^{-1} (asymmetric stretching vibrations of (Al)O–H), 3090 cm^{-1} (symmetric stretching vibrations of (Al)O–H), 2094 cm^{-1} (combination vibration of AlO–H), 1975 cm^{-1} (combination vibration of AlO–H), 1636 cm^{-1} (bending mode of adsorbed H_2O), 1453 cm^{-1} (O–H vibration of hydration water), 1078 cm^{-1} (symmetric stretching vibration of Al–O–H), 1153 cm^{-1} (asymmetric stretching vibration of Al–O–H), and bands at 746 cm^{-1}, 620 and 496 cm^{-1} (the vibration mode of <AlO_6>) [35–37]. The spectrum of the nanocomposite with $x = 2.5\%$; Fig. 3b is very similar to that of Al–LH, except for the bands at 3453 cm^{-1}, and 1018 cm^{-1} might be ascribed to the stretching vibration of the hydroxyl groups in the layered structure [38]. The spectrum of MWCNTs exhibits bands at 3856 and 3746 cm^{-1} denote the OH stretching of a hydroxyl group attached to MWCNTs walls [39], 3421 cm^{-1} could be assigned due to the hydroxyl group (–OH). This band may be due to both water and also the functional groups (–OH) resulting from the chemical treatment during the purification and functionalization processes, respectively [40]. Additional bands also seem in the MWCNTs spectrum at 2916 cm^{-1} (asymmetric stretching of C–H), 2858 cm^{-1} (symmetric stretching of C–H), 2381 cm^{-1} (the stretching of C≡C), 1704 cm^{-1} (the stretching of –COOH group), 1644 cm^{-1} (C=C stretching vibration), 1518 cm^{-1} (the stretching of C=C), 1062 cm^{-1} (C–C stretching vibration), and 1431 cm^{-1} (the C–H bend of the alkyl chain) [39,41]. The appearance of a band around 1160 cm^{-1} proves that the band observed around 1704 cm^{-1} corresponds to the carboxylic group due to the interaction between the –CO bending and –OH stretching [40]. As could be noted from Fig. (3a–d), nearly similar spectra were obtained for all nanocomposites. It may be due to the small amounts of MWCNTs combined into the Al–LH matrix. It is also noted that band positions corresponding to MWCNTs as well as Al–LH are shifted in the spectra of the obtained nanocomposites. All these findings demonstrate the presence of interaction between MWCNTs and Al–LH.

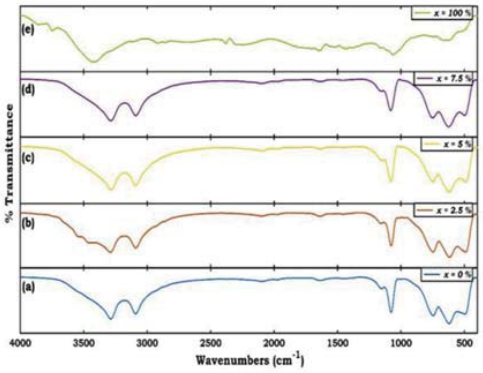

Fig. 3. (a-e): FTIR Spectra of (1-x) Al–LH + (x) MWCNTs nanocomposites with $x = 0$, 2.5, 5, 7.5 and 100 wt%.

3.3. High-resolution transmission electron microscopy (HRTEM)

The microstructure of the samples was examined using High-resolution transmission electron microscopy and illustrated in Fig. 4. The Al–LH is observed as typical layers arranged in the Z-direction (3-D arrangement). These layers are shown to have a regular geometric form. From a closer look, the orthorhombic symmetry is clarified which is in line with the X-ray data analysis. For $x = 2.5\%$, the layers are seen to be stacked and possess nearly the same crystallinity. Increasing MWCNTs content, the orthorhombic symmetry of the layers is preserved while the 3-dimensional arrangement is altered and/or randomness is started. At $x = 7.5\%$, some of the layers are remarked from a side view besides the ones oriented in a top one. The MWCNTs are obviously clear to be of inner diameter 6.47 nm, outer one 31.26 nm and more than 3 walls are countable. From a higher magnification and zooming in, the view is slightly different with more details. The layers are proved to have very good crystallinity and the layer thickness is measured. The stacking here is obvious due to electrostatic attraction. The MWCNTs at $x = 5$ and 7.5% are anchored on the layer surface without changing the geometry. The interlayer

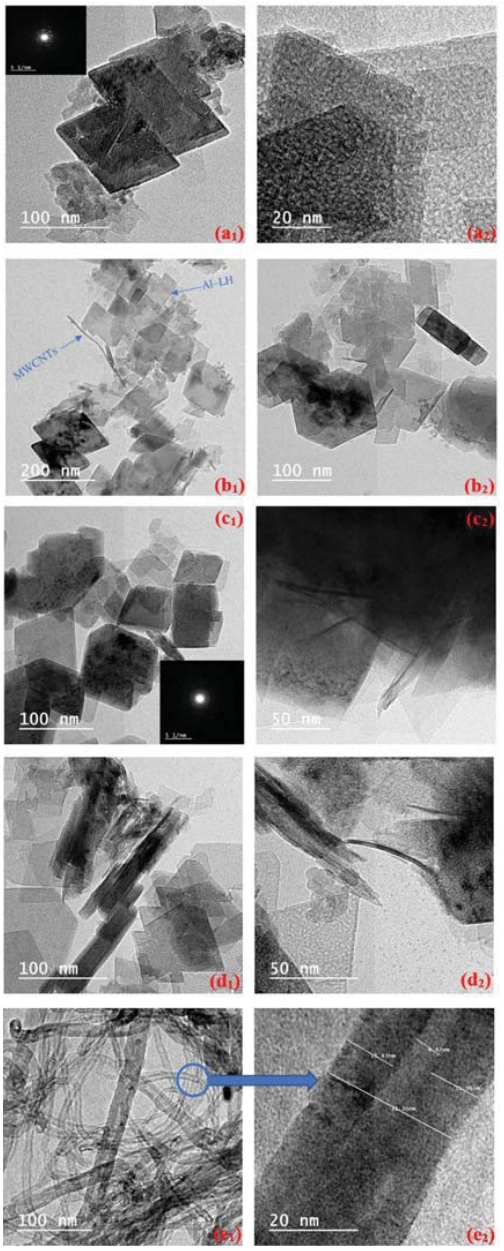

Fig. 4. HRTEM micrographs of (1-*x*) Al–LH + (*x*) MWCNTs nanocomposites; (a) $x = 0$, (b) $x = 2.5$, (c) $x = 5$, (d) $x = 7.5$, (e) $x = 100$ wt%.

space is enlarged in the case more than the parent LH i.e. without MWCNTs. The amount of the later is very small in the micrographs where the content here, in this case, is considered to be low. The insets of the figure represent the selected area electron diffraction (SAED) where clear rings are noticed and get sharper for the nanocomposite indicating better crystallinity.

3.4. Field emission scanning electron microscopy (FESEM)

FESEM is used to examine the surface morphology of the investigated samples either LH, MWCNTs or the prepared nanocomposites. Fig. 5 showed the excellent homogeneous surface of the LH in the orthorhombic form with the cracked rough surface. From a deep look, the LH orthorhombic crystals are well defined and the surface becomes clearer. The crystals are seen from the top. Some morphology and crystalline features of the grains are remarked in $x = 2.5\%$. The microcrack formation on the layer's surface is a common characteristic trend either for LH or nanocomposites. For $x = 5\%$, the microcracks and pores are deeper and the grain arrangement is altered. At $x = 7.5\%$, the growth of MWCNTs on the LH surface is simply clarified and the grown nanotubes are oriented to bridge between the different grains. Generally, the LH and their nanocomposites resemble to a dehydrated clay surface which recommends them for water decontamination and versatile water treatment. The MWCNTs are seen to be formed in an ordered oriented tubular form bundled together in a homogenous manner. The spaghetti-like shape is observed with diameter ≈ 40 nm and of micron length. Zooming out the nanotubes of carbon are likely to form silk ball morphology.

The micrographs of FESEM were processed by Gwyddion 2.50 software to investigate the surface roughness of the investigated nanocomposites [42,43]. The file extensions were jpg without further calibrations. After that, selected areas in the micrographs were cropped to avoid graph boundaries using the software. Thereafter a 3D graph was created for each micrograph. The resolution of the micrographs was kept at 1500×1100 pixel to facilitate the comparison. The roughness parameters were calculated using the same software. Fig. 6a–e shows the dependence of surface roughness on MWCNTs content. The micrographs elucidated that the roughness arises as a function of *x*. Table 3 shows that the maximum height of the roughness (R_t) increased from 0.38 to 0.64 μm. Also, the root means square roughness (R_q) increased from 68 to 119 nm for the investigated nanocomposites from $x = 0.0$ to 100 wt %.

3.5. Zeta potential and size

Zeta potential is an important physicochemical parameter that estimates the surface charge and colloidal stability of nanosuspensions [44]. The large positive values of the zeta potential assure the stability of the nanocomposites in water at the ambient conditions [45]. From the data in Table 4, all nanocomposites are positively charged with different values of potential. The zeta size indicated the hydrodynamic diameter of the nanocomposites under investigation where it varied depending on MWCNTs concentration. The largest one is at the concentration ($x = 5\%$) of MWCNTs. These large values are due to the particles existing in a layered form which is in line with the observation of HRTEM Fig. 4.

3.6. BET surface area analysis

The N_2 adsorption-desorption isotherms for all prepared samples are shown in Fig. 7. All samples showed a typical type IV isotherm with a clear H3 hysteresis loop which is a common feature of layered materials [46]. The values of BET surface area, pore width,

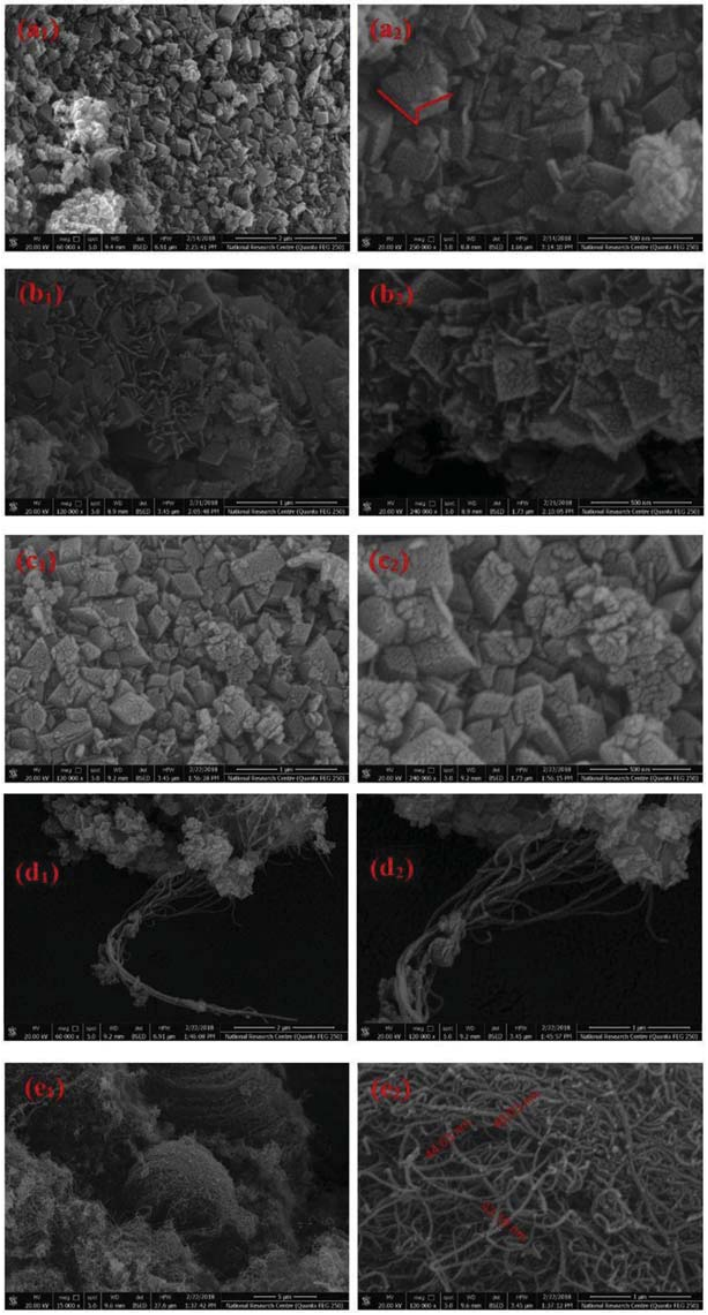

Fig. 5. FESEM micrographs of (1-*x*) Al–LH + (*x*) MWCNTs nanocomposites; (a) $x = 0$, (b) $x = 2.5$, (c) $x = 5$, (d) $x = 7.5$, (e) $x = 100$ wt%.

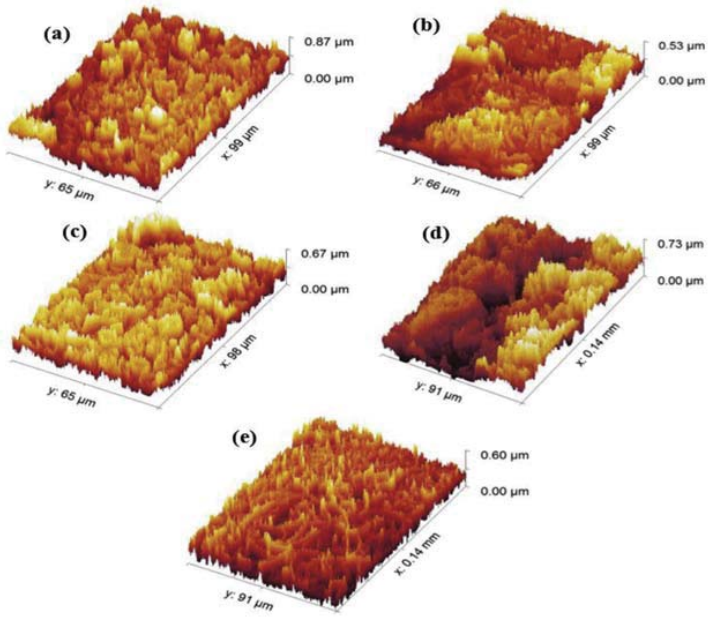

Fig. 6. Roughness of the investigated samples (1-x) Al–LH + (x) MWCNTs; (a) $x = 0$, (b) $x = 2.5$, (c) $x = 5$, (d) $x = 7.5$, and (e) $x = 100$ wt%.

Table 3
Roughness parameters for the investigated nanocomposites of (1-x) Al–LH + (x) MWCNTs with $x = 0$, 2.5, 5, 7.5, and 100 wt%.

x (wt.%)	R_a (nm)	R_t (µm)	R_q (nm)
0	96.55 ± 11.30	0.6363 ± 0.07298	119.7 ± 13.51
2.5	54.43 ± 4.58	0.3778 ± 0.04618	68.11 ± 5.815
5	79.41 ± 7.18	0.5058 ± 0.05053	97.53 ± 7.876
7.5	91.63 ± 19.53	0.5249 ± 0.1003	113.6 ± 23.94
100	66.58 ± 4.98	0.4432 ± 0.04629	81.75 ± 5.95

and pore volume are summarized in Table 5. The BET surface area of the 2.5 wt % sample enjoyed the largest value of surface area due to the addition of the MWCNTs and its smallest crystallite size. With further increase in the MWCNTs concentration, the crystallite size increased and the surface area is decreased. These results agree with those reported [47]. The difference between the values obtained for MWCNTs ($x = 100\%$) and the other nanocomposites originated from the morphological feature of the MWCNTs. The measured pore width is nearly about 3.3 nm and the samples are classified as mesoporous [46].

Table 4
The values of zeta potential and zeta size as a function x for the nanocomposites (1-x) Al–LH + (x) MWCNTs with $x = 0$, 2.5, 5, 7.5 and 100 wt%.

x (wt.%)	Zeta potential (mV)	Zeta Size (nm)
0	34.63	443.43
2.5	32.00	349.70
5	33.40	487.97
7.5	38.23	388.53
100	2.06	14770

3.7. Thermal properties

3.7.1. Thermal gravimetric analysis

Thermal gravimetric analysis (TGA-DTG) was carried out for the investigated nanocomposites from room temperature up to 700 °C to quantify the improvement in their thermal stability as shown in Fig. 8. The pure Al–LH and the nanocomposite with $x = 2.5\%$ suffer three steps decomposition Fig. 8 a, b which is typically shown by Layered Hydroxides. Their first weight loss step was observed at about 55.69 °C and 67.99 °C with weight losses of 1.365% and 3.690% respectively. This step is ascribed to the loss of adsorbed moisture. The second weight loss step was observed at 215.39 °C and 243.10 °C with weight losses of 2.904% and 6.486% respectively. This step is ascribed to the dehydration of the interlayer water existing in the Al–LH. The final step was observed at 463.63 °C and 460.28 °C with weight losses of 16.35% and 13.54% respectively which corresponds to the removal of water due to the dehydroxylation of the brucite-like layers. In this step, metal hydroxide was converted to Al oxide [48].

The nanocomposites with $x = 5$ and 7.5% undergo dual steps decomposition Fig. 8c, d with the first step (54.41 °C and 67.13 °C with weight losses of 6.370% and 7.058%) being attributed to the loss of adsorbed moisture. The final stages (480.18 °C and 473.27 °C with weight losses of 16.87% and 17.08%) are due to the complete formation of the oxide [39]. Increasing MWCNTs concentration ($x = 5$ and 7.5%) leads to the improvement of the thermal stability of the investigated nanocomposites. The reason for this improvement is that MWCNTs are turning around themselves to form silk ball-like as seen in FESEM micrographs Fig. 5e. This finding is in line with the crystallite size as with increasing the later the decomposition takes place at higher temperatures [48,49].

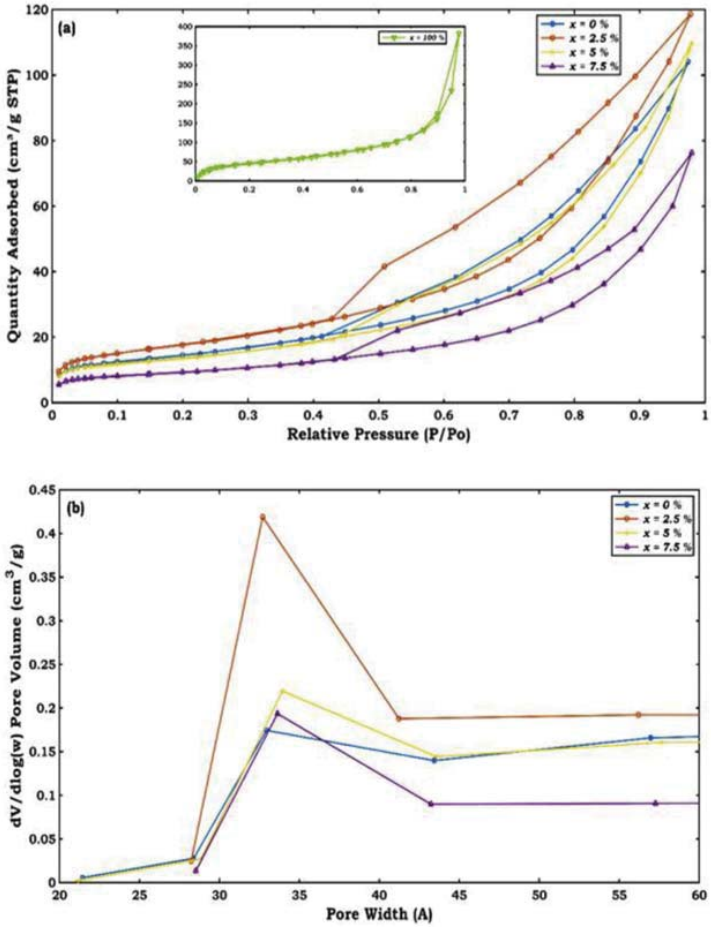

Fig. 7. N_2 adsorption-desorption isotherms (a) and corresponding pore size distribution curves (b) of the Al–LH and MWCNTs nanocomposites.

Table 5
The values of surface area, pore width and pore volume as a function *x* for the nanocomposites (1-*x*) Al–LH + (*x*) MWCNTs with $x = 0$, 2.5, 5, 7.5 and 100 wt%.

x (wt.%)	Surface Area (m^2/g)	Pore width (nm)	Pore volume (cm^3/g)	Classification	Type
0	51.86	3.29	0.17	Mesoporous	IV
2.5	63.36	3.27	0.42	Mesoporous	IV
5	48.28	3.39	0.22	Mesoporous	IV
7.5	32.60	3.36	0.19	Mesoporous	IV
100 (MWCNTs)	169.38	–	–	–	–

3.7.2. Differential scanning calorimetry analysis

Differential scanning calorimetry (DSC) was performed for the prepared nanocomposites from room temperature up to 700 °C as depicted in Fig. 9. All nanocomposites exhibit an exothermic decomposition reaction with the formation of the oxide at high decomposition temperatures. The exothermic peaks take place at 502.51 °C, 513.41 °C, 507.51 °C and 507.54 °C for the nanocomposites with $x = 0$, 2.5, 5 and 7.5 wt% respectively. Only the nanocomposite with $x = 2.5$ wt% exhibits an endothermic decomposition reaction with the dehydration of the interlayer water existing in the Al–LH at 248.69 °C.

3.7.3. Activation energy

The kinetics of a reaction is usually governed by the activation

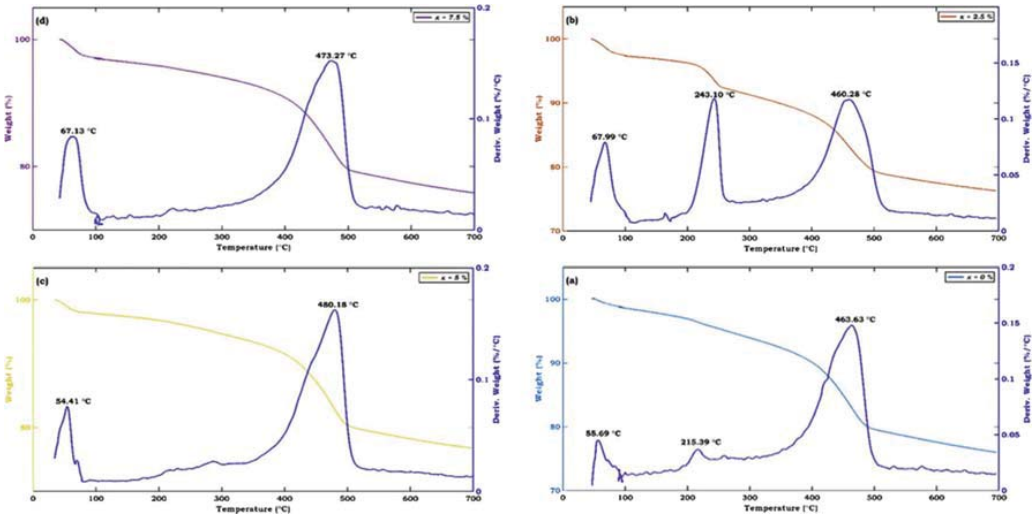

Fig. 8. TGA-DTG thermograms of (1-*x*) Al–LH + (*x*) MWCNTs nanocomposites; (a) $x = 0$, (b) $x = 2.5$, (c) $x = 5$, (d) $x = 7.5$ wt%.

energy barrier that is required to be overcome. A low rate of thermal degradation implies an increased thermal stability of the material, which should be accompanied by a rise in activation energy. Thermal gravimetric data is utilized to calculate the activation energy based on three methods; Coats-Redfern, Horowitz–Metzger, and Broido.

3.7.3.1. Coats-Redfern method. This method obeys the equation [50,51]:

$$\boldsymbol{ln}\left[\frac{-(1-\alpha)}{\boldsymbol{T^2}}\right] = \boldsymbol{ln}\left(\frac{\boldsymbol{AR}}{\boldsymbol{\beta E}}\right) - \frac{\boldsymbol{E_a}}{\boldsymbol{RT}} \tag{7}$$

where: α is the fraction of sample which decomposed at time t, T is the absolute temperature (Kelvin), A is the Arrhenius pre-exponential factor, R is the universal gas constant (8.314 J/mol K), β is the heating rate which equals dT/dt and E_a is the activation energy.

By plotting the dependence $\ln\left[\frac{-(1-\alpha)}{T^2}\right]$ versus $\frac{1000}{T}$ for each sample, a straight line was obtained and from the slope, the activation energy can be calculated as:

$$\boldsymbol{E_a} = -\boldsymbol{R} \times \boldsymbol{slope} \tag{8}$$

3.7.3.2. Horowitz–Metzger method. Horowitz–Metzger equation was formulated as [52,53]:

$$\boldsymbol{ln}\left[\boldsymbol{ln}(1-\alpha)^{-1}\right] = \frac{\boldsymbol{E_a\theta}}{\boldsymbol{RT_s^2}} \tag{9}$$

where: R is the universal gas constant, $\theta = T - T_s$ while T is the given temperature and T_s is the temperature at a reaction step from DTG curve.

By plotting the dependence $\ln[ln(1-\alpha)^{-1}]$ versus θ for each sample, a straight line was obtained and from the slope, the activation energy can be calculated as:

$$\boldsymbol{E_a} = \boldsymbol{slope} \times \boldsymbol{R} \times \boldsymbol{T_s^2} \tag{10}$$

3.7.3.3. Broido method. Broido introduces a model to calculate the activation energy using the equation:

$$\boldsymbol{ln}\left[\boldsymbol{ln}\left(\frac{1}{\boldsymbol{Y}}\right)\right] = -\left(\frac{\boldsymbol{E_a}}{\boldsymbol{R}}\right)\frac{1}{\boldsymbol{T}} + \boldsymbol{constant} \tag{11}$$

where: Y is the fraction of the nondegraded material and calculated as:

$$\boldsymbol{Y} = \frac{\boldsymbol{m_t - m_f}}{\boldsymbol{m_i - m_f}} \tag{12}$$

where: m_t, m_i and m_f are the residual weight at temperature t, initial weight and final weight of the sample, respectively. By plotting the dependence $\ln\left[ln\left(\frac{1}{Y}\right)\right]$ versus $\frac{1}{T}$ for each sample, a straight line was obtained and from the slope, the activation energy can be calculated [51,54] as:

$$\boldsymbol{E_a} = -\boldsymbol{R} \times \boldsymbol{slope} \tag{13}$$

Fig. 10a shows the activation energy values (E_a) of the investigated samples by Coats – Redfern, Horowitz–Metzger and Broido methods. From a common view, they have the same trend but with different values. The activation energy of the nanocomposites with $x = 5$ and 7.5% are found to be greater than that of the pure Al–LH and the nanocomposite with $x = 2.5\%$ which indicates that better thermal stability can be achieved with increasing MWCNTs concentration. This finding is in line with the crystallite size as the later gives the same trend as shown in Fig. 10 [48,49]. From these results, it can be concluded that thermal stability of these nanocomposites

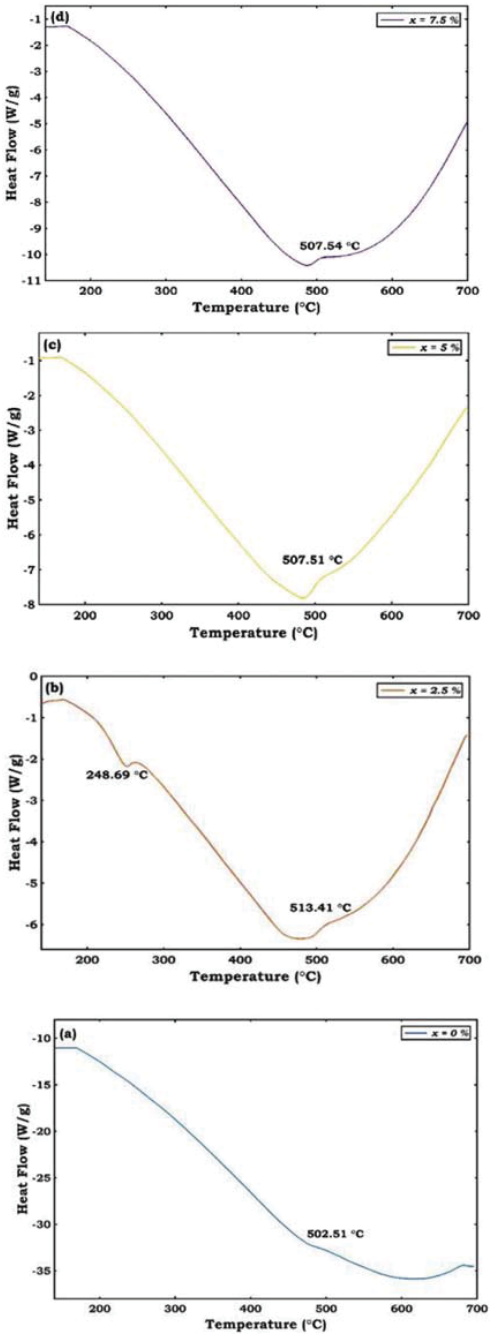

Fig. 9. DSC curves of (1-*x*) Al–LH + (*x*) MWCNTs nanocomposites; (a) $x = 0$, (b) $x = 2.5$, (c) $x = 5$, (d) $x = 7.5$ wt%.

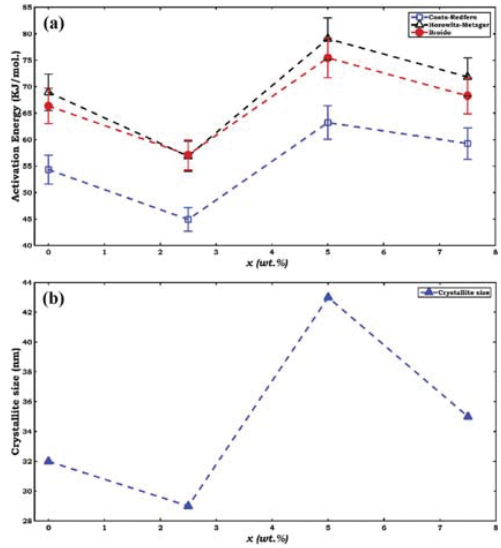

Fig. 10. Values of the activation energy using Coats – Redfern, Horowitz - Metzger, and Broido methods (a) and the crystallite size (b) for the nanocomposites with $x = 0$, 2.5, 5, and 7.5 wt%; Lines are guide for eyes.

Table 6
The values of longitudinal velocity (V_L), and shear velocity (V_S) as a function *x* for the nanocomposites (1-*x*) Al–LH + (*x*) MWCNTs with $x = 0$, 2.5, 5 and 7.5 wt%.

x (wt.%)	V_L (m/s)	V_S (m/s)
0	910	780
2.5	812	551
5	732	569
7.5	711	551

was improved with increasing MWCNTs concentration making them a good candidate for use in high-temperature applications in the thermal range from the room temperature up to 480 °C.

3.8. Mechanical properties

The longitudinal velocity V_L and shear velocity V_S for the investigated nanocomposites were measured using the ultrasonic pulse-echo technique and summarized in Table 6.

Using the values in Tables (2) and (6), several parameters including the longitudinal modulus (L), Rigidity modulus (G), Poisson's ratio (σ), Bulk modulus (B), and Young's modulus (E) were calculated using the relations below [33,55] and the results are

Table 7
The elasticity parameters L, G, B, σ and E in addition to the calculated Vickers microhardness H_v as a function *x* for the nanocomposites (1-*x*) Al–LH + (*x*) MWCNTs with $x = 0$, 2.5, 5 and 7.5 wt%.

x (wt.%)	L (GPa)	G (GPa)	B (MPa)	σ	E (GPa)	H_v (GPa)
0	1.34	0.99	27.38	- 0.88	0.23	0.91
2.5	0.97	0.45	372.91	0.07	0.96	0.13
5	1.19	0.72	232.13	−0.26	1.06	0.37
7.5	0.93	0.56	184.52	−0.25	0.83	0.28

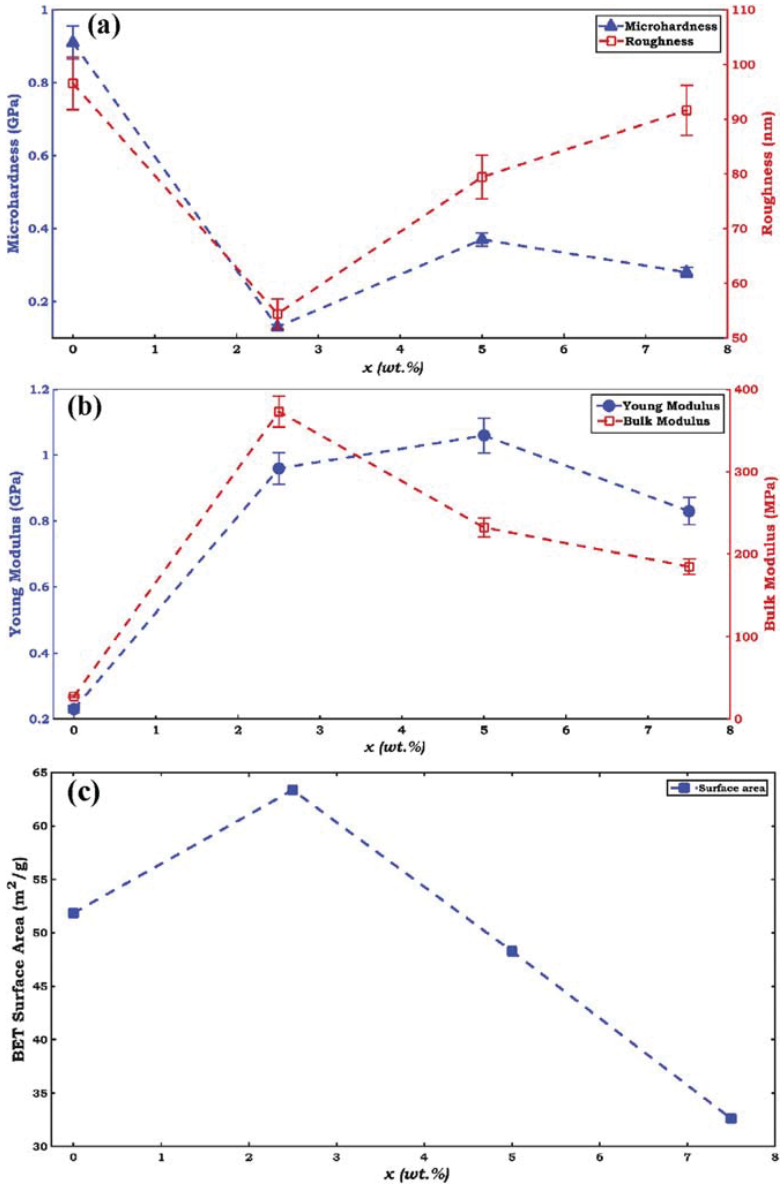

Fig. 11. (a) dependence of microhardness and roughness on MWCNTs content, (b) Young's modulus and Bulk's modulus on MWCNTs content, and (c) BET surface area on MWCNTs content; Lines are guide for eyes.

displayed in Table 7:

$$\mathbf{L} = \rho_{exp}\, \mathbf{V}_L^2 \tag{14}$$

$$\mathbf{G} = \rho_{exp}\, \mathbf{V}_S^2 \tag{15}$$

$$\mathbf{B} = \mathbf{L} - \frac{4}{3}\boldsymbol{G} \tag{16}$$

$$\boldsymbol{\sigma} = \frac{3\boldsymbol{B} - 2\boldsymbol{G}}{6\boldsymbol{B} + 2\boldsymbol{G}} \tag{17}$$

$$\mathbf{E} = (1 + \boldsymbol{\sigma})2\boldsymbol{G} \tag{18}$$

The calculated Vickers microhardness (H_V) is related to Young's modulus (E), and Poisson's ratio (σ) by the following relation and the results are displayed in Table 7.

$$\boldsymbol{H_V} = \frac{(1 - 2\boldsymbol{\sigma})\boldsymbol{E}}{6(1 + \boldsymbol{\sigma})} \tag{19}$$

From the data in Table 7, the pure Al–LH and the nanocomposites with $x = 5$ and 7.5% exhibit a negative Poisson's ratio where it expands under the applied stress. Therefore, these nanocomposites are auxetic materials [42,56]. It is demonstrated that the pure Al–LH displays higher negative ratio than that of other samples which leads to high indentation resistance. This expectation is matched well with the microhardness results. This is obvious result due to the existence of interlayer spacing in the layered hydroxide.

The calculated Vickers microhardness decreased with the addition of MWCNTs in the investigated nanocomposites, with negative deviation from the trend at the concentration of $x = 2.5$ wt % as shown in Fig. 11a. This finding is in line with the porosity as the later gives the opposite trend. The negative deviation is ascribed to lower roughness and also to the lower density of that nanocomposite.

On the other hand, Young's modulus is improved by 417%, 460%, and 360% compared to neat Al–LH with 2.5, 5 and 7.5 wt% MWCNTs respectively. Moreover, the Bulk modulus is enhanced by 14, 9 and 7 times compared to that of the pure Al–LH with 2.5, 5 and 7.5 wt% MWCNTs respectively as clarified in Fig. 11b. This large improvement is related to the strong interfacial interaction between MWCNTs with Al-LH. The nanocomposites with $x = 2.5$ and 5 wt% exhibit larger improvement than that of the nanocomposite with $x = 7.5$ wt% which are related to their larger surface area as clarified in Fig. 11c. From these findings, these nanocomposites are a strongly recommended as 3D hybrid nanofillers.

4. Conclusion

Multiwalled carbon nanotubes were successfully synthesized using chemical vapor deposition method. Al − Layered Hydroxide and MWCNTs nanocomposites; (1-x) Al–LH + (x) MWCNTs, $0.0 \leq x \leq 1$; were successfully synthesized using citrate nitrate assisted hydrothermal method. All the nanocomposites exhibit large positive values of the zeta potential which assure their stability in water at the ambient conditions. The dehydrated clay surface of the prepared nanocomposites recommends them for water decontamination and versatile water treatment. The 2.5 wt % sample has the largest value of surface area as well as its smallest crystallite size. Moreover, the measured pore width of the samples is nearly about 3.3 nm and they are classified as mesoporous. The nanocomposites with $x = 5$ and 7.5% exhibit better thermal stability with increasing MWCNTs concentration and increasing the crystallite size making them a good candidate for high-temperature applications. The calculated Poisson's ratio showed an auxetic behavior. The calculated microhardness was found to be in line with the calculated Poisson's ratio and the porosity as the later gives the opposite trend. Moreover, a nice correlation was established between calculated microhardness and the roughness. The Young's modulus is improved by 417%, 460%, and 360% compared to neat Al–LH with 2.5, 5 and 7.5 wt% MWCNTs respectively. Moreover, the Bulk modulus is enhanced by 14, 9 and 7 times compared to that of the pure Al–LH with 2.5, 5 and 7.5 wt% MWCNTs respectively. This large improvement is related to the strong interfacial interaction between MWCNTs with Al–LH. Owing to the superior mechanical properties of these samples ($x = 2.5$ and 5 wt %), the discussed results may suggest a new methodology for the fabrication of reinforcing nanofiller.

Data availability

The raw data required to reproduce these findings are available to download from [10.6084/m9.figshare.7257218]. The processed data required to reproduce these findings are available to download from [10.6084/m9.figshare.7257218].

Acknowledgments

The authors are grateful to Prof. A.A. Farghali and Eng. Yasser. M. Gadel Hak Materials science and nanotechnology Department, Faculty of Postgraduate Studies for Advanced Sciences (PSAS), Beni-Suef University, Egypt for their help and contribution to improve the quality of our work.

References

[1] P. Mangiacapra, M. Raimondo, L. Tammaro, V. Vittoria, M. Malinconico, P. Laurienzo, Nanometric dispersion of a Mg/Al layered double hydroxide into a chemically modified polycaprolactone, Biomacromolecules 8 (2007) 773–779.
[2] L. Yang, Nanotechnology-enhanced Orthopedic Materials: Fabrications, Applications and Future Trends, Woodhead Publishing, 2015.
[3] F. Lv, C. Li, Y. Ma, Z. Sun, R. Li, Z. Zhao, Fabrication of step-by-step drug release system both sensitive to magnetic field and temperature based on layered double hydroxides and PNIPAM, Nanotechnology 30 (2018) 55103.
[4] F. Beigi, M.S.S. Mousavi, F. Manteghi, M. Kolahdouz, Doped nafion-layered double hydroxide nanoparticles as a modified ionic polymer metal composite sheet for a high-responsive humidity sensor, Appl. Clay Sci. 166 (2018) 131–136, https://doi.org/10.1016/j.clay.2018.09.006.
[5] H. Wang, S. Tan, R. Song, Effect of trace chloride on the char formation and flame retardancy of the LLDPE filled with NiAl-layered double hydroxides, Fire Mater. (2018) 1–11, https://doi.org/10.1002/fam.2674.
[6] J. Cui, Z. Zhou, A. Xie, Q. Wang, S. Liu, J. Lang, C. Li, Y. Yan, J. Dai, Facile preparation of grass-like structured NiCo-LDH/PVDF composite membrane for efficient oil–water emulsion separation, J. Membr. Sci. 573 (2019) 226–233, https://doi.org/10.1016/j.memsci.2018.11.064.
[7] S.A.A. Moaty, A.A. Farghali, R. Khaled, Preparation, characterization and antimicrobial applications of Zn-Fe LDH against MRSA, Mater. Sci. Eng. C 68 (2016) 184–193, https://doi.org/10.1016/j.msec.2016.05.110.
[8] S.A.A. Moaty, A.A. Farghali, M. Moussa, R. Khaled, Remediation of waste water by Co–Fe layered double hydroxide and its catalytic activity, J. Taiwan Inst. Chem. Eng. 71 (2017) 441–453, https://doi.org/10.1016/j.jtice.2016.12.001.
[9] S. Yuan, Y. Li, Q. Zhang, H. Wang, ZnO/Mg-Al layered double hydroxides as strongly adsorptive photocatalysts, Res. Chem. Intermed. 35 (2009) 685.
[10] L. Unnikrishnan, S. Mohanty, S.K. Nayak, N. Singh, Synthesis and characterization of polysulfone/clay nanocomposite membranes for fuel cell application, J. Appl. Polym. Sci. 124 (2012) E309–E318.
[11] X. Wang, Y. Zhao, E. Tian, J. Li, Y. Ren, Graphene oxide-based polymeric membranes for water treatment, Adv. Mater. Interfaces. 5 (2018) 1–20, https://doi.org/10.1002/admi.201701427.
[12] L. Burk, M. Walter, A.C. Asmacher, M. Gliem, M. Moseler, R. Mülhaupt, Mechanochemically aminated multilayer graphene for carbon/polypropylene graft polymers and nanocomposites 13 (2019) 286–301.
[13] L.M. Clayton, A.K. Sikder, A. Kumar, M. Cinke, M. Meyyappan, T.G. Gerasimov, J.P. Harmon, Transparent poly(methyl methacrylate)/single-walled carbon nanotube (PMMA/SWNT) composite films with increased dielectric constants,

Adv. Funct. Mater. 15 (2005) 101–106, https://doi.org/10.1002/adfm.200305106.
[14] A. Miranda, N. Barekar, B.J. McKay, MWCNTs and their use in Al-MMCs for ultra-high thermal conductivity applications: a review, J. Alloys Compd. 774 (2019) 820–840, https://doi.org/10.1016/j.jallcom.2018.09.202.
[15] K.A. Wepasnick, B.A. Smith, K.E. Schrote, H.K. Wilson, S.R. Diegelmann, D.H. Fairbrother, Surface and structural characterization of multi-walled carbon nanotubes following different oxidative treatments, Carbon N. Y. 49 (2011) 24–36, https://doi.org/10.1016/j.carbon.2010.08.034.
[16] B. Pradhan, S.K. Srivastava, R. Ananthakrishnan, A. Saxena, Preparation and characterization of exfoliated layered double hydroxide/silicone rubber nanocomposites, J. Appl. Polym. Sci. 119 (2011) 343–351, https://doi.org/10.1002/app.32614.
[17] B. Pradhan, S.K. Srivastava, A.K. Bhowmick, A. Saxena, Effect of bilayered stearate ion-modified Mg-Al layered double hydroxide on the thermal and mechanical properties of silicone rubber nanocomposites, Polym. Int. 61 (2012) 458–465, https://doi.org/10.1002/pi.3218.
[18] S. Mallakpour, M. Hatami, Condensation Polymer/layered Double Hydroxide NCs: Preparation, Characterization, and Utilizations, Elsevier Ltd, 2017, https://doi.org/10.1016/j.eurpolymj.2017.03.015.
[19] M.N. Tchoul, W.T. Ford, G. Lolli, D.E. Resasco, S. Arepalli, Effect of mild nitric acid oxidation on dispersability, size, and structure of single-walled carbon nanotubes, Chem. Mater. 19 (2007) 5765–5772, https://doi.org/10.1021/cm071758l.
[20] C. Gao, S. Muthukrishnan, W. Li, J. Yuan, Y. Xu, A.H.E. Müller, Linear and hyperbranched glycopolymer-functionalized carbon nanotubes: synthesis, kinetics, and characterization, Macromolecules 40 (2007) 1803–1815, https://doi.org/10.1021/ma062238z.
[21] A. Ramírez-Jiménez, S. Hernández-López, E. Vigueras-Santiago, Conductive polymeric composites based on multiwalled carbon nanotubes and linseed oil functionalized and cross-linked with diacetylenes from propargyl alcohol, J. Nanomater. 2015 (2015), https://doi.org/10.1155/2015/531249.
[22] H. Wang, X. Xiang, F. Li, Facile synthesis and novel electrocatalytic performance of nanostructured Ni-Al layered double hydroxide/carbon nanotube composites, J. Mater. Chem. 20 (2010) 3944–3952, https://doi.org/10.1039/b924911g.
[23] M.M. Shaijumon, N. Bejoy, S. Ramaprabhu, Catalytic growth of carbon nanotubes over Ni/Cr hydrotalcite-type anionic clay and their hydrogen storage properties, Appl. Surf. Sci. 242 (2005) 192–198, https://doi.org/10.1016/j.apsusc.2004.08.014.
[24] H. Wang, X. Xiang, F. Li, Hybrid ZnAl-LDH/CNTs nanocomposites: noncovalent assembly and enhanced photodegradation performance, AIChE J. 56 (2010) 768–778, https://doi.org/10.1002/aic.12020.
[25] B. Du, Z. Fang, The preparation of layered double hydroxide wrapped carbon nanotubes and their application as a flame retardant for polypropylene, Nanotechnology 21 (2010) 315603, https://doi.org/10.1088/0957-4484/21/31/315603.
[26] X. Xiang, L. Bai, F. Li, Formation and catalytic performance of supported ni nanoparticles via self-reduction of hybrid NiAl-LDH/C composites, AIChE J. 56 (2010) 2934–2945, https://doi.org/10.1002/aic.12189.
[27] Y.F. Lan, J.J. Lin, Observation of carbon nanotube and clay micellelike microstructures with dual dispersion property, J. Phys. Chem. A. 113 (2009) 8654–8659, https://doi.org/10.1021/jp9026805.
[28] S. Huang, H. Peng, W.W. Tjiu, Z. Yang, H. Zhu, T. Tang, T. Liu, Assembling exfoliated layered double hydroxide (LDH) nanosheet/carbon nanotube (CNT) hybrids via electrostatic force and fabricating nylon nanocomposites, J. Phys. Chem. B 114 (2010) 16766–16772, https://doi.org/10.1021/jp1087256.
[29] J.A. Schwarz, C. Contescu, A. Contescu, Methods for preparation of catalytic materials, Chem. Rev. 95 (1995) 477–510.
[30] M. Bahgat, A.A. Farghali, W. El Rouby, M. Khedr, M.Y. Mohassab-Ahmed, Adsorption of methyl green dye onto multi-walled carbon nanotubes decorated with Ni nanoferrite, Appl. Nanosci. 3 (2013) 251–261, https://doi.org/10.1007/s13204-012-0127-3.
[31] A.A. Farghali, A.H. Zaki, M.H. Khedr, Hydrothermally synthesized TiO2 nanotubes and nanosheets for photocatalytic degradation of color yellow sunset, Int. J. Adv. Res. 2 (2014) 285–291.
[32] A.A. Farghali, M.H. Khedr, S.I. El-Dek, A.E. Megahed, Synthesis and multifunctionality of (CeO2-NiO) nanocomposites synthesized via sonochemical technique, Ultrason. Sonochem. 42 (2018) 556–566, https://doi.org/10.1016/j.ultsonch.2017.12.011.
[33] W. Malaeb, H. Basma, M.M. Barakat, R. Awad, Investigation of the mechanical properties of GdBa2Cu3O7−δ added with nanosized ferrites ZnFe2O4 and CoFe2O4 using ultrasonic measurement, J. Supercond. Nov. Magn. 30 (2017) 3595–3602, https://doi.org/10.1007/s10948-016-3863-x.
[34] B.D. Cullity, S.R. Stock, Elements of X-Ray Diffraction, Pearson Education, Limited, 2013.
[35] T. Wang, S. Liu, Green synthesis and photoluminescence property of AlOOH nanoflakes, Powder Technol. 294 (2016) 280–283, https://doi.org/10.1016/j.powtec.2016.02.046.
[36] Y. Feng, W. Lu, L. Zhang, X. Bao, B. Yue, Y. Iv, X. Shang, One-step synthesis of hierarchical cantaloupe-like AlOOH superstructures via a hydrothermal route, Cryst. Growth Des. 8 (2008) 1426–1429, https://doi.org/10.1021/cg7007683.
[37] U. Janosovits, G. Ziegler, U. Scharf, A. Wokaun, Structural characterization of intermediate species during synthesis of Al2O3-aerogels, J. Non-Cryst. Solids 210 (1997) 1–13.
[38] J. Qu, X. He, B. Wang, L. Zhong, L. Wan, X. Li, S. Song, Q. Zhang, Synthesis of Li-Al layered double hydroxides via a mechanochemical route, Appl. Clay Sci. 120 (2016) 24–27, https://doi.org/10.1016/j.clay.2015.11.017.
[39] P. Sen, G. Pugazhenthi, Synergistic effect of dual nanofillers (MWCNT and Ni-Al LDH) on the electrical and thermal characteristics of polystyrene nanocomposites, J. Appl. Polym. Sci. 135 (2018) 46513, https://doi.org/10.1002/app.46513.
[40] M. Bahgat, A.A. Farghali, W.M.A. El Rouby, M.H. Khedr, Synthesis and modification of multi-walled carbon nano-tubes (MWCNTs) for water treatment applications, J. Anal. Appl. Pyrolysis 92 (2011) 307–313, https://doi.org/10.1016/j.jaap.2011.07.002.
[41] S. Roy, S.K. Srivastava, V. Mittal, Noncovalent assembly of carbon nanofiber – layered double hydroxide as a reinforcing hybrid filler in thermoplastic polyurethane – nitrile butadiene rubber blends, 2016, pp. 1–10, https://doi.org/10.1002/app.43470, 43470.
[42] S.F. Mansour, S.I. El-Dek, M.K. Ahmed, Physico-mechanical and morphological features of zirconia substituted hydroxyapatite nano crystals, Sci. Rep. 7 (2017) 1–21, https://doi.org/10.1038/srep43202.
[43] S.F. Mansour, S.I. El-dek, M. Ismail, M.K. Ahmed, Structure and cell viability of Pd substituted hydroxyapatite nano particles, Biomed. Phys. Eng. Express. 4 (2018), 045008, https://doi.org/10.1088/2057-1976/aac07c.
[44] S. Honary, F. Zahir, Effect of zeta potential on the properties of nano - drug delivery systems - a review (Part 2), Trop. J. Pharm. Al Res. 12 (2013) 265–273, https://doi.org/10.4314/tjpr.v12i2.19.
[45] P. Saikia, R.L. Goswamee, The effect of strength of bases and temperature on the synthesis of Zn-Al layered double hydroxides by a non-aqueous 'soft chemical' sol-gel method and formation of high surface area mesoporous ZnAl$_2$O$_4$ spinel, ChemistrySelect 3 (2018) 7619–7626, https://doi.org/10.1002/slct.201801094.
[46] M. Thommes, K. Kaneko, A.V. Neimark, J.P. Olivier, F. Rodriguez-Reinoso, J. Rouquerol, K.S.W. Sing, Physisorption of gases, with special reference to the evaluation of surface area and pore size distribution (IUPAC Technical Report), Pure Appl. Chem. 87 (2015) 1051–1069, https://doi.org/10.1515/pac-2014-1117.
[47] T. Tsukada, H. Segawa, A. Yasumori, K. Okada, Crystallinity of boehmite and its effect on the phase transition temperature of alumina, J. Mater. Chem. 9 (1999) 549–563.
[48] X. Bokhimi, J.A. Toledo-Antonio, M.L. Guzmán-Castillo, F. Hernández-Beltrán, Relationship between crystallite size and bond lengths in boehmite, J. Solid State Chem. 159 (2001) 32–40, https://doi.org/10.1006/jssc.2001.9124.
[49] Y. Li, J. Liu, Z. Jia, Fabrication of boehmite AlOOH nanofibers by a simple hydrothermal process, Mater. Lett. 60 (2006) 3586–3590, https://doi.org/10.1016/j.matlet.2006.03.083.
[50] A.W. Coats, J.P. Redfern, Kinetic parameters from thermogravimetric data, Nature 201 (1964) 68.
[51] A.M. Hezma, I.S. Elashmawi, E.M. Abdelrazek, A. Rajeh, M. Kamal, Enhancement of the thermal and mechanical properties of polyurethane/polyvinyl chloride blend by loading single walled carbon nanotubes, Prog. Nat. Sci. Mater. Int. 27 (2017) 338–343, https://doi.org/10.1016/j.pnsc.2017.06.001.
[52] L. a. a. Pérez-Maqueda, P.E.E. Sánchez-Jiménez, J.M.M. Criado, Evaluation of the integral methods for the kinetic study of thermally stimulated processes in polymer science, Polymer (Guildf). 46 (2005) 2950–2954, https://doi.org/10.1016/j.polymer.2005.02.061.
[53] M.E. Islam, M.M. Rahman, M. Hosur, S. Jeelani, Thermal stability and kinetics analysis of epoxy composites modified with reactive polyol diluent and multiwalled carbon nanotubes, J. Appl. Polym. Sci. 132 (2015) 1–11, https://doi.org/10.1002/app.41558.
[54] A. Broido, A simple, sensitive graphical method of treating thermogravimetric analysis data, J. Polym. Sci. 2 Polym. Phys. 7 (1969) 1761–1773, https://doi.org/10.1002/pol.1969.160071012.
[55] S.F. Mansour, M.A. Abdo, S.I. El-Dek, Improvement of physico-mechanical properties of Mg–Zn nanoferrites via Cr3+doping, J. Magn. Magn Mater. 422 (2017) 105–111, https://doi.org/10.1016/j.jmmm.2016.07.049.
[56] G.N. Greaves, A.L. Greer, R.S. Lakes, T. Rouxel, Poisson's ratio and modern materials, Nat. Mater. 10 (2011) 823–837, https://doi.org/10.1038/nmat3134.

خطة البحث

للتسجيل لدرجة الماجستير في العلوم الهندسية في الفيزياء الهندسية

اسم الباحث: المهندس / محمد عقيل شوقى عبد الوهاب

معيد بقسم العلوم الهندسية الأساسية - كلية الهندسة ببنها - جامعة بنها

عنوان البحث:

" تحضير و دراسة الخواص الفيزيائية لبعض المتراكبات النانومترية "

ملخص البحث:

تطوير المواد النانومترية هو واحد من أهم التطورات في مجال العلوم. المواد النانومترية هى المواد التي تحتوي علي بعد واحد علي الأقل في نطاق النانو ، والذي يعطيها خصائص فيزيائية وكيميائية غير عادية. المتراكبات النانومترية ذو الطبقات تمثل فئة محدده من المواد متعددة الأغراض التي حصلت علي العديد من الاعتبارات في السنوات الاخيره. وتسمح تلك المتراكبات النانومترية بتقدم التطبيقات المبتكرة في الصناعة بالاضافه إلى انها تمثل بديلا ابتكاريا للبحوث الخاصة بالمواد الجديدة. ويشمل الاستخدام المحتمل للمتراكبات النانومترية ذو الطبقات الاجهزه الضوئية ، والاغشيه الذكية ، وكاشفات الكيمياء الحيوية والكيميائية ، والمحفزات الجديدة ، وأجهزه الفصل ، والاجهزه الكترونيه الذكية بالاضافه إلى بعض المواد دمج السيراميك و البوليمرات ، الخ. التفاعلات القوية والتشتت المتجانس مع المصفوفات هي المشكلة الأكثر اهميه للمتراكبات النانومترية ذو الطبقات . وعلاوة علي ذلك ، لم تجر دراسات بشان تحضير متراكبات نانومترية من هيدروكسيد الألمنيوم ذو الطبقات والأنابيب النانومترية الكربونية متعددة الجدران. وبدافع من هذا ، فاننا سوف نركز عملنا علي تحضير متراكبات نانومترية من هيدروكسيد الألمنيوم ذو الطبقات والأنابيب النانومترية الكربونية متعددة الجدران ودراسة خصائصها الفيزيائية للتطبيقات المحتملة.

خطة البحث:

١. تحضير المتراكبات النانومترية باستخدام الطريقة الهيدروحرارية.

٢. التأكد من التركيب البللورى و طبيعة الروابط الكيميائية للمتراكبات النانومترية باستخدام تقنية حيود الأشعة السينية و الأشعة تحت الحمراء .
٣. استخدام المجهر الألكترونى عالى الدقة للتأكد من البنية الدقيقة.
٤. استخدام المسح المجهرى الألكترونى للتأكد من مورفولوجي و تضاريس السطح.
٥. قياس جهد زيتا لجميع المتراكبات النانومترية.
٦. قياس مساحة السطح لجميع المتراكبات النانومترية.
٧. قياس الخصائص الفيزيائية لجميع المتراكبات النانومترية.

لجنة الإشراف:

أ.م .د/ سماء امام محمود الدق ( )
أستاذ مساعد بقسم علوم المواد و تكنولوجيا النانو
كلية الدراسات العليا للعلوم المتقدمة – جامعة بنى سويف

د/ محمد مصطفى محمد الفحام ( )
مدرس بقسم العلوم الهندسية الاساسية
كلية الهندسة ببنـــها – جامـعة بنـــها

٢. التأكد من التركيب البللورى و طبيعة الروابط الكيميائية للمتراكبات النانومترية باستخدام تقنية حيود الأشعة السينية و الأشعة تحت الحمراء .

٣. استخدام المجهر الألكترونى عالى الدقة للتأكد من البنية الدقيقة.

٤. استخدام المسح المجهرى الألكترونى للتأكد من مورفولوجي و تضاريس السطح.

٥. قياس جهد زيتا لجميع المتراكبات النانومترية.

٦. قياس مساحة السطح لجميع المتراكبات النانومترية.

٧. قياس الخصائص الفيزيائية لجميع المتراكبات النانومترية.

لجنة الإشراف:

أ.م .د/ سماء أمام محمود الدق ( )

أستاذ مساعد بقسم علوم المواد و تكنولوجيا النانو

كلية الدراسات العليا للعلوم المتقدمة – جامعة بنى سويف

د/ محمد مصطفى محمد الفحام ( )

مدرس بقسم العلوم الهندسية الاساسية

كلية الهندسة ببنـــها – جامـعة بنـــها

ملخص البحث باللغة العربية

لقد تم تحضير الأنابيب النانومترية الكربونية متعددة الجدران باستخدام طريقة ترسيب البخار الكيميائي. كما تم تحضير متراكبات نانومترية من هيدروكسيد الألمنيوم ذو الطبقات والأنابيب النانومترية الكربونية متعددة الجدران باستخدام الطريقة الهيدروحرارية. وتم التأكد من التركيب البللورى و طبيعة الروابط الكيميائية للمتراكبات النانومترية باستخدام تقنية حيود الأشعة السينية و الأشعة تحت الحمراء. وبدا البناء الطبقى لها تحت المجهر الألكترونى عالى الدقة ، ولوحظت المورفولوجي و تضاريس السطح باستخدام المسح المجهرى الألكترونى. وعلاوة علي ذلك، تم قياس جهد زيتا و مساحة السطح للمتراكبات المعدة و أوضحت القياسات تغير فى خصائصها عند تغيير تركيز الأنابيب النانومترية الكربونية متعددة الجدران. وأكد التحليل الحراري للمتراكبات النانومترية ثباتها الحراري خلال المدى من درجه حرارة الغرفة إلى ٤٨٠ درجه مئوية اعتمادا علي تركيز الأنابيب النانومترية الكربونية متعددة الجدران. وكشفت النتائج التي تم الحصول عليها تحسين جميع الخواص الميكانيكية مع زيادة تركيز الأنابيب النانومترية الكربونية متعددة الجدران.

قامت اللجنة الموقعة أدناه بتحكيم الرسالة تحت عنوان

تحضير و دراسة الخواص الفيزيائية لبعض المتراكبات النانومترية

المقدمة من

محمد عقيل شوقى عبدالوهاب

بكالوريوس الهندسة و التكنولوجيا فى الهندسة الكهربية – كلية الهندسة ببنها – جامعة بنها (٢٠١١)

كجزء من متطلبات الحصول علي درجة الماجستير في العلوم الهندسية في الفيزياء الهندسية

أُعتمدت و أُجيزت من لجنة الحكم و المناقشة

أ.د/ جمال عبد الناصر مدبولى أستاذ متفرغ بقسم الفيزياء نائب رئيس جامعة القاهرة السابق كلية العلوم – جامعة القاهرة	**(رئيساً)**
أ.م.د/ محمود فتحى محمود حسن أستاذ مساعد بقسم العلوم الهندسية الأساسية كلية الهندسة ببنها – جامعة بنها	**(عضواً)**
أ.م.د/ سماء أمام محمود الدق أستاذ مساعد بقسم علوم المواد و تكنولوجيا النانو كلية الدراسات العليا للعلوم المتقدمة – جامعة بنى سويف	**(عضواً)**

أُعتمدت من قسم العلوم الهندسية الاساسية

أ.د/ السيد علي إبراهيم فؤاد **(رئيس القسم)**

أُعتمدت من الدراسات العليا

أ.د/ هشام محمد البطش **(وكيل الكلية للدراسات العليا)**

أُعتمدت من الكلية

أ.د/ عارف محمد سليمان **(عميد الكلية)**

جامعة بنها
كلية الهندسة ببنها

قامت اللجنة الموقعة أدناه بتحكيم الرسالة تحت عنوان

تحضير و دراسة الخواص الفيزيائية لبعض المتراكبات النانومترية

المقدمة من

محمد عقيل شوقى عبدالوهاب

بكالوريوس الهندسة و التكنولوجيا فى الهندسة الكهربية – كلية الهندسة ببنها – جامعة بنها (٢٠١١)

كجزء من متطلبات الحصول علي درجة الماجستير في العلوم الهندسية في الفيزياء الهندسية

أُعتمدت و أُجيزت من لجنة الحكم و المناقشة

أ.د/ جمال عبد الناصر مدبولى أستاذ متفرغ بقسم الفيزياء نائب رئيس جامعة القاهرة السابق كلية العلوم – جامعة القاهرة	**(رئيساً)**
أ.م.د/ محمود فتحى محمود حسن أستاذ مساعد بقسم العلوم الهندسية الأساسية كلية الهندسة ببنها – جامعة بنها	**(عضواً)**
أ.م.د/ سماء أمام محمود الدق أستاذ مساعد بقسم علوم المواد و تكنولوجيا النانو كلية الدراسات العليا للعلوم المتقدمة – جامعة بنى سويف	**(عضواً)**

أُعتمدت من قسم العلوم الهندسية الاساسية

أ.د/ السيد علي إبراهيم فؤاد **(رئيس القسم)**

أُعتمدت من الدراسات العليا

أ.د/ هشام محمد البطش **(وكيل الكلية للدراسات العليا)**

أُعتمدت من الكلية

أ.د/ عارف محمد سليمان **(عميد الكلية)**

جامعة بنها
كلية الهندسة ببنـها
قسم العلوم الهندسية الاساسية

تحضير و دراسة الخواص الفيزيائية لبعض المتراكبات النانومترية

الرسالة مقدمة للحصول علي درجة الماجستير في العلوم الهندسية في الفيزياء الهندسية

إعداد

محمد عقيل شوقى عبد الوهاب

بكالوريوس الهندسة و التكنولوجيا فى الهندسة الكهربية – كلية الهندسة ببنها – جامعة بنها (٢٠١١)

المشرفون

أ.م.د/ سماء أمام محمود الدق
أستاذ مساعد بقسم علوم المواد و تكنولوجيا النانو
كلية الدراسات العليا للعلوم المتقدمة
جامعة بنى سويف

د/ محمد مصطفى محمد الفحام
مدرس بقسم العلوم الهندسية الاساسية
كلية الهندسة ببنـها
جامعة بنها

بنـها ٢٠١٩